We are IntechOpen, the world's leading publisher of Open Access books
Built by scientists, for scientists

Model Reference Control of Human-Operated Mobile Robot for Object Transportation

Naoki Uchiyama and Tatsuhiro Hashimoto
Toyohashi University of Technology
Japan

1. Introduction

Robotic systems are expected to engage in various types of tasks, such as housework, nursing and welfare work, and industrial work done by skilled workers. Although fully automated robots are desirable, it appears difficult to produce such robots from the viewpoints of cost efficiency and the technologies available currently. Human-operated robotic systems are a good compromise, and hence are widely studied. Objectives of these robots include extending human mechanical power (Kazerooni & Steger, 2006), providing precise and smooth operation for human workers in difficult tasks (Bettini et al., 2001) (Peshkin et al., 2001), and executing a task in remote or hazardous environment (Anderson & Spong, 1989) (Lawrence, 1993).

In human-operated robotics systems, controllers are required to incorporate the human operator's command and compensate for the operator's mistakes without reducing the ease of operation. For this purpose we propose a model reference control approach, in which the reference model generates a desired trajectory according to the operator's input and constraints such as collision avoidance. This approach is applied to a two wheeled mobile robot that transports an object. This type of robot has various applications in many areas. Because transporting objects is a fundamental task of robotic systems, we realize a function to prevent slip and tumble of the transported object even when the human operator makes mistakes during operation. Fixing the transported object to the robotic system to prevent the object from tumbling requires extra time to transport the object and reduces the operational ease. This is because fixing is a time-consuming and inconvenient task. In particular, supposing that the robot is operated by elderly or disabled people, this function will be necessary for providing easy and safe operations. In addition, a collision avoidance function is implemented by the proposed model reference approach.

Many studies have been conducted into the obstacle avoidance of mobile robots (Bonnafous & Lefebvre, 2004) (Fox et al., 1997) (Khatib, 1986) (Ögren, P. & Leonard, 2005). Most of the existing approaches provide sophisticated algorithms that minimize some objective functions, such as required time to reach the goal and moving distances. However, these methods assume the fully automatic motion of robotic systems, and hence, the human operator's commands cannot generally be incorporated in real-time. In addition, tumble avoidance of the transported object is not considered in current methods. In the case of human-operated robot, a simple algorithm for real-time calculation, rather than optimization, is required because the time-consuming processing required may reduce the robot's operativity. The effectiveness of the proposed approach is demonstrated by experimental results, where ten unskilled operators operate the robot with/without the proposed method.

2. Human-Operated Mobile Robot

In this chapter, we consider a control problem of a general type two-wheeled mobile robot that transports an object as shown in Fig. 1. Human operators are enabled to handle the robot using control sticks. They can give command signals for driving forces of each wheel u_l and u_r by inclining left and right sticks, respectively. The magnitudes of driving forces are proportional to the inclined angles of the sticks. The robot dynamics is given as follows:

$$I\ddot{\phi} = \left(u_r - u_l\right)L, \tag{1}$$

$$M\dot{v} = u_r + u_l, \tag{2}$$

where I and M are the inertia and the mass of the robot, respectively. The symbol L is the half distance between the two wheels. The symbols v and ϕ are the translational speed and rotation angle of the robot, respectively. The slip of wheels is not considered in this study. The shape of the robot is assumed as a circle for simplicity. Distance sensors to detect obstacles are located symmetrically with respect to the centerline parallel to the translational direction of the robot as shown in Fig. 1. The distance from the center of the robot to each sensor is denoted by R. The located direction of each sensor from a line that links wheel centers is denoted by ψ_i. Note that ψ_i has a positive value.

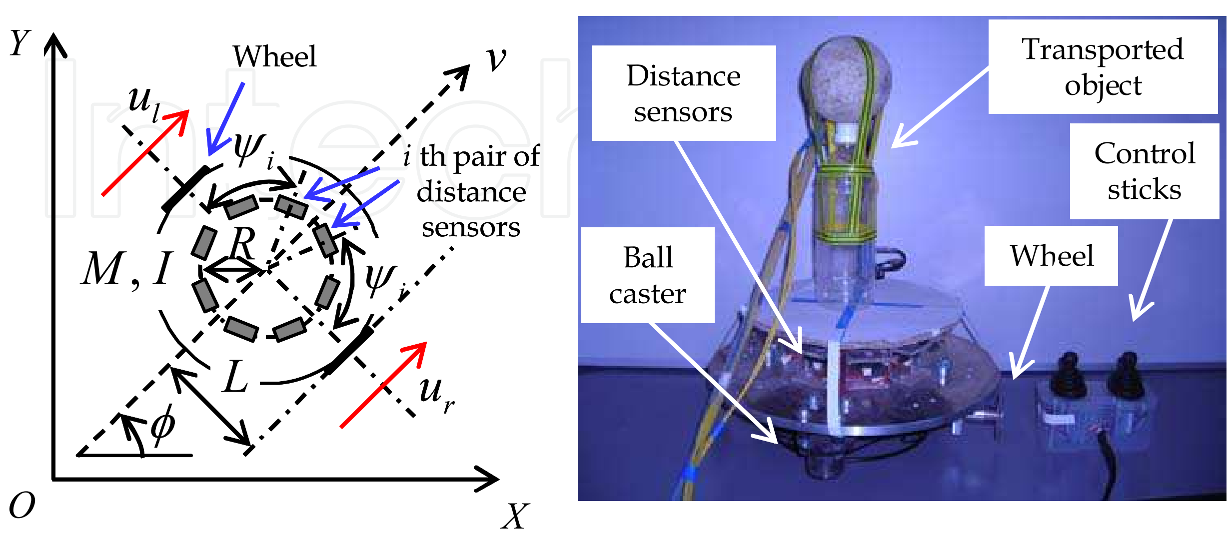

Fig. 1. Human –operated mobile robot that transports an object

3. Controller Design

3.1 Model reference control for obstacle avoidance

To consider the nonholonomicity of the robot and incorporate the operator's command, we propose an obstacle avoidance algorithm based on the model reference approach as shown in Fig. 2, where the reference model generates the desired angles of each wheel, $\dot{\theta}_{ld}$ and $\dot{\theta}_{rd}$, according to the operator's command input and distance sensor information. The reference model, which has a similar dynamics with the mobile robot except for an obstacle avoidance function, is given as follows:

$$I\ddot{\phi} + C_{\phi}\dot{\phi} = \left(u_r - u_l\right)L + \sum_{i=1}^{m}\frac{\alpha_i}{\sqrt[n]{d_{ri}}} - \sum_{i=1}^{m}\frac{\alpha_i}{\sqrt[n]{d_{li}}}, \quad (3)$$

$$M\dot{v} + C_v v = u_r + u_l - \sum_{i=1}^{m}\frac{\beta_i}{\sqrt[n]{d_{ri}}} - \sum_{i=1}^{m}\frac{\beta_i}{\sqrt[n]{d_{li}}}, \quad (4)$$

where C_{ϕ} and C_v are the virtual viscous friction coefficients. The viscous friction terms generally exist due to the actuator viscous friction and increase the system stability. We use these terms to increase the control system stability as shown in the analysis in Section 3.2. The symbols d_{li} and d_{ri} are the distances between sensors at angle ψ_i and the obstacle, where the subscripts l and r mean that the sensor is located at the left and right wheel side, respectively. Only sensors that are located in the same half side of the robot body with moving direction v are active. The symbol m denotes the half number of the active sensors. The last two terms on the right-hand side of Eq. (3) give an effect of steering. The magnitude of the steering depends on the distances to the obstacle d_{li} and d_{ri}. The last two terms on the right-hand side of Eq. (4) play a role of brake. The magnitude of braking force also depends on the distances to the obstacle. The symbols α_i and β_i are constant parameters for changing the effects of these steering- and brake-like functions. The n th roots of the distances are employed in these terms for varying the response to the obstacle, and their effects are shown in Fig. 3. Decreasing the value of n increases the effects of steering- and brake-like functions. The reference motion of the robot is obtained by numerically integrating Eqs. (3) and (4). The values of $\dot{\phi}$ and v in Eqs. (3) and (4) are converted into wheel reference signals as follows:

$$R_w\dot{\theta}_{ld} = v - L\dot{\phi}, \; R_w\dot{\theta}_{rd} = v + L\dot{\phi}, \quad (5)$$

where R_w is the radius of wheel.

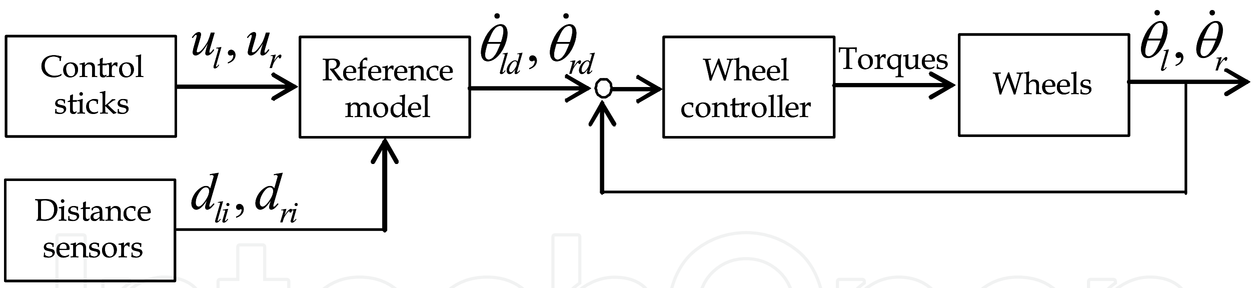

Fig. 2. Block diagram of model reference control approach

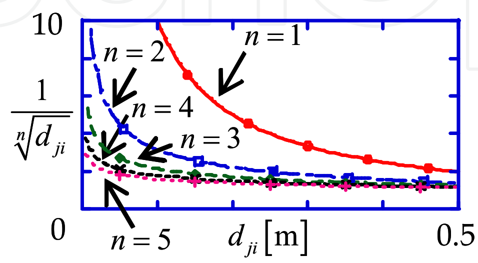

Fig. 3. Properties of functions for obstacle avoidance

3.2 Stability analysis based on linear model

This section presents a stability analysis based on a linear model of the proposed reference model in Eqs. (3) and (4). In this analysis, we consider the case in Fig. 4, where the two parallel walls are obstacles. It is assumed that the mobile robot moves almost along the centerline between the two walls with a velocity $v = v_0 + v_s$, where v_0 is a desired constant and v_s is a small-sized variable. Because the mobile robot is in an almost straight line motion with a constant velocity, it is reasonable to assume that the input from the operator satisfies the relation $u_r + u_l \simeq C_v v_0$ and $u_r \simeq u_l$. We also assume that both the shift from the centerline x_s and the inclination from the lateral line ϕ_s in Fig. 4 are small-sized variables.

The distance between each sensor and walls are given by

$$d_{li} = \frac{D + x_s}{\cos(\psi_i - \phi_s)} - R, \quad d_{ri} = \frac{D - x_s}{\cos(\psi_i + \phi_s)} - R \tag{6}$$

where D is the half distance between the walls. Because ϕ_s and x_s are small-sized variables, the following linear approximation is reasonable:

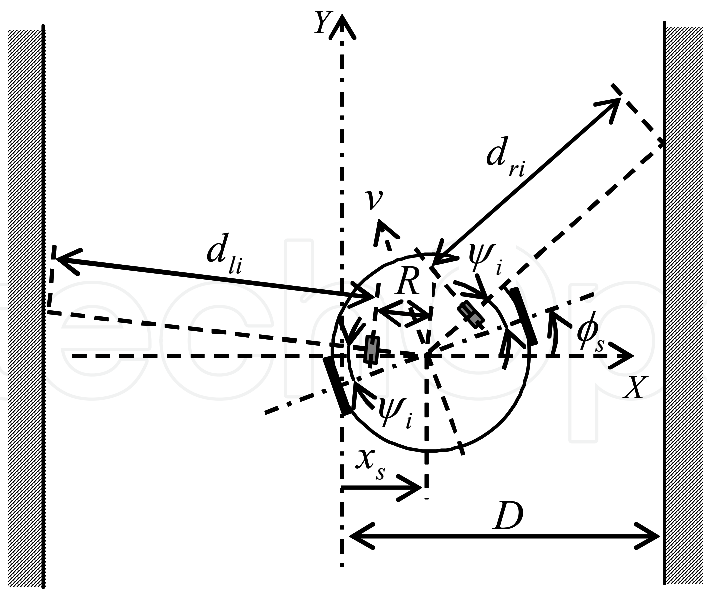

Fig. 4. Schematic for stability analysis

$$d_{li} = a_i - b_i\phi_s + c_i x_s\,,\; d_{ri} = a_i + b_i\phi_s - c_i x_s\,, \tag{7}$$
$$a_i = \frac{D}{\cos\psi_i} - R\,,\; b_i = \frac{D\sin\psi_i}{\cos^2\psi_i}\,,\; c_i = \frac{1}{\cos\psi_i}$$

Note that a_i, b_i and c_i are positive constants.

The following linear approximation is also reasonable because ϕ_s and x_s have small magnitudes:

$$\frac{1}{\sqrt[n]{d_{ji}}} = -p_i d_{ji} + q_i, \quad j = l, r, \tag{8}$$

where p_i and q_i are positive constants.

Equation (3) is written as follows from Eqs. (6) - (8) and the assumptions given above:

$$I\ddot{\phi}_s + C_\phi\dot{\phi}_s = \sum_{i=1}^{m}\alpha_i p_i\left(-2b_i\phi_s + 2c_i x_s\right) \tag{9}$$

The dynamics on x_s is given as:

$$\dot{x}_s = -v\sin\phi_s \simeq -\left(v_0 + v_s\right)\phi_s \simeq -v_0\phi_s \tag{10}$$

Equation (4) is linearized as:

$$M\dot{v}_s + C_v v_s = 2\sum_{i=1}^{m} \beta_i \left(p_i a_i - q_i \right) \tag{11}$$

Because Eq. (11) has no coupling term on ϕ_s and x_s, we consider Eqs. (9) and (10) in the stability analysis. It should be noted that Eq. (11) is stable because M and C_v are positive and the right-hand side is bounded.

Defining a vector $z = \left[\phi_s, \dot{\phi}_s, x_s \right]^T$, we have the following linear dynamics from Eqs. (9) and (10):

$$\dot{z} = Az \tag{12}$$

$$A = \begin{bmatrix} 0 & 1 & 0 \\ \dfrac{-2}{I}\sum_{i=1}^{m} \alpha_i p_i b_i & \dfrac{-C_\phi}{I} & \dfrac{2}{I}\sum_{i=1}^{m} \alpha_i p_i c_i \\ -v_0 & 0 & 0 \end{bmatrix}$$

The characteristic polynomial of the system Eq. (12) is

$$\left| sI - A \right| = s^3 + \frac{C_\phi}{I} s^2 + \frac{2}{I}\sum_{i=1}^{m} \alpha_i p_i b_i s + \frac{2v_0}{I}\sum_{i=1}^{m} \alpha_i p_i c_i \,. \tag{13}$$

Because all the coefficients of the right-hand side of Eq. (13) are positive, the stability condition is given by:

$$\frac{C_\phi}{I}\sum_{i=1}^{m} \alpha_i p_i b_i - v_0 \sum_{i=1}^{m} \alpha_i p_i c_i > 0 \,. \tag{14}$$

From Eqs. (7) and (14), the following sufficient condition for the stability is derived:

$$C_\phi D \sin\psi_i - I v_0 \cos\psi_i > 0, \quad i = 1, \cdots, m \,. \tag{15}$$

By assigning the coefficient C_ϕ such that Eq. (15) is satisfied, the stability of the linearized dynamics in Eq. (12) is guaranteed.

3.3 Object transportation control

Because transporting objects is a fundamental task of robotic systems, we include a function to prevent slip and tumble of the transported object in the reference model block in Fig. 2 even when the human operator makes mistakes during operation. Fixing the transported

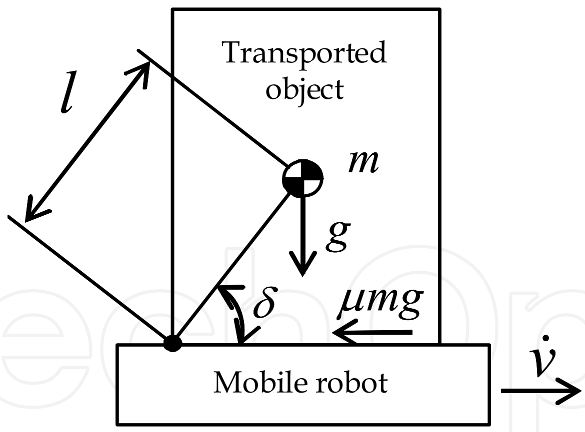

Fig. 5. Derivation of conditions to avoid slip and tumble

object to the robotic system to prevent the object from slip and tumble requires extra time to transport the object and reduces the operational ease.
Because the value of M in Eq. (4) does not necessarily have an exact value of the mass of robot, we change this value in real time to adjust the reference acceleration to prevent the object from slip and tumble. Increasing this value reduces the magnitude of the reference acceleration.
In this study, we assume that the slip and tumble of the transported object is caused mainly by the translational acceleration, although the acceleration normally includes the centrifugal and the Coriolis terms. The slip of the object is prevented if the inertial force is smaller than the static friction force as follows:

$$m|\dot{v}| \leq \mu m \mathrm{g}\,, \tag{15}$$

where m is the mass of the transported object, μ is the static friction coefficient of the contacting surface between the object and the robot, and g is the gravitational acceleration. Figure 5 is the schematic of this relation. Hence, we have the allowable acceleration $\dot{v}_{s\max}$ to avoid the slip as follows:

$$\dot{v}_{s\max} = \mu \mathrm{g}\,. \tag{16}$$

Next, we consider the allowable acceleration to avoid the tumble. We assume that the object starts to rotate at the end point of the contacting surface with the robot as shown in Fig. 5. Considering the equation around the center of rotation, we obtain the following condition for preventing the object from starting to tumble.

$$ml|\dot{v}|\sin\delta \leq ml\,\mathrm{g}\cos\delta, \tag{17}$$

where δ is the angle from the contacting surface line to the center of gravity of the transported object, and l is the distance between centers of rotation and gravity, as shown in Fig. 5. Hence, we obtain the acceleration limit for avoiding the tumble $\dot{v}_{t\max}$ as follows:

$$\dot{v}_{t\max} = g\cot\delta \tag{18}$$

From Eqs. (16) and (18), the allowable acceleration to avoid the slip and tumble is given as:

$$\dot{v}_{\max} = \min\left(\dot{v}_{s\max}, \dot{v}_{t\max}\right) \tag{19}$$

To avoid the tumble, we propose to adjust the mass coefficient $M(t)$ as follows from Eq. (4) :

$$M(t) = \begin{cases} \dfrac{1}{\dot{v}_{\max}}\left\{-C_v v + u_r + u_l - \sum_{i=1}^{m}\dfrac{\beta_i}{\sqrt[n]{d_{ri}}} - \sum_{i=1}^{m}\dfrac{\beta_i}{\sqrt[n]{d_{li}}}\right\}, & \text{if } |\dot{v}| > \dot{v}_{\max}, \\ M_0, & \text{otherwise.} \end{cases} \tag{20}$$

where M_0 is the initial value of the mass coefficient $M(t)$.

4. Experiment

The effectiveness of the proposed controller is experimentally verified in a corridor-like space shown in Fig. 6. Parameter values for the experiment are given in Table 1. Parameters for obstacle avoidance α_i, β_i and n are determined in a trial and error manner. DC servo motors (20 [W]) are employed for each wheel motion. Rotary encoders (500 [PPR]) attached to the motors are used for measuring the position and orientation of the robot. Infrared distance sensors, whose measurable ranges are 4 - 30 [cm], are employed to measure the distance to the obstacle.

To verify the effect for the operational easiness, ten unskilled persons (students) are employed to operate the robot with the transported object $(\delta = 75\,[\text{deg}])$ in Fig. 1 under the following conditions:

(a1) Manual control
(a2) Control with the obstacle avoidance function presented in section 3.2.
(a3) Control with the obstacle avoidance and the tumble avoidance functions in section 3.3.

Parameter	Value	Parameter	Value	Parameter	Value
I	0.056 [kgm^2]	C_ϕ	3.0 [Nms/rad]	α_i	4 [Nm$^{5/4}$]
M	5.4 [kg]	C_v	10.0 [Ns/m]	β_i	10.0[Nm$^{1/4}$]
R	0.11 [m]	R_w	0.029 [m]	n	4
L	0.17 [m]	m	2		

Table 1. Parameter values in experiment

In (a3), only the tumble is considered because $\dot{v}_{t\max} \gg \dot{v}_{s\max}$ in this experiment.

Figures 7 - 9 show the obtained robot trajectories by one operator under conditions (a1) – (a3), respectively. In case (a1), as negative values of u_l and u_l are shown in Fig. 7 (a), backward motions were required to pass through the course. The backward motion is confirmed in Fig. 7 (d). In addition, both collision and tumble occurred in this case. The latter is caused by a large magnitude of acceleration as shown in Fig. 7 (b).

In case (a2), although u_l and u_l were almost constant during operation as shown in Fig. 8 (a), the robot changed its orientation ϕ in Fig. 8 (c) by the obstacle avoidance function. In addition, no backward motion was required as shown in Fig. 8 (d). However, a large magnitude of the acceleration in Fig. 8 (b) caused the tumble of the transported object.

In case (a3), the robot was enabled to smoothly pass through the course by an almost constant inputs in Fig. 9 (a) without requiring a large magnitude of acceleration as shown in Fig. 9 (b).

Table 2 summarizes experimental results by ten unskilled operators (students), where no collision occurs in cases (a2) and (a3), and no tumble occurs in case (a3), for all operators. Figure 10 summarizes the control time required to pass through the course. The control time is largely reduced for almost all operators by the model reference control approach, because they do not have to consider the obstacle or tumble avoidance during operation. The control time in case (a3) increases little compared to case (a2), although the acceleration magnitude is reduced to avoid the tumble.

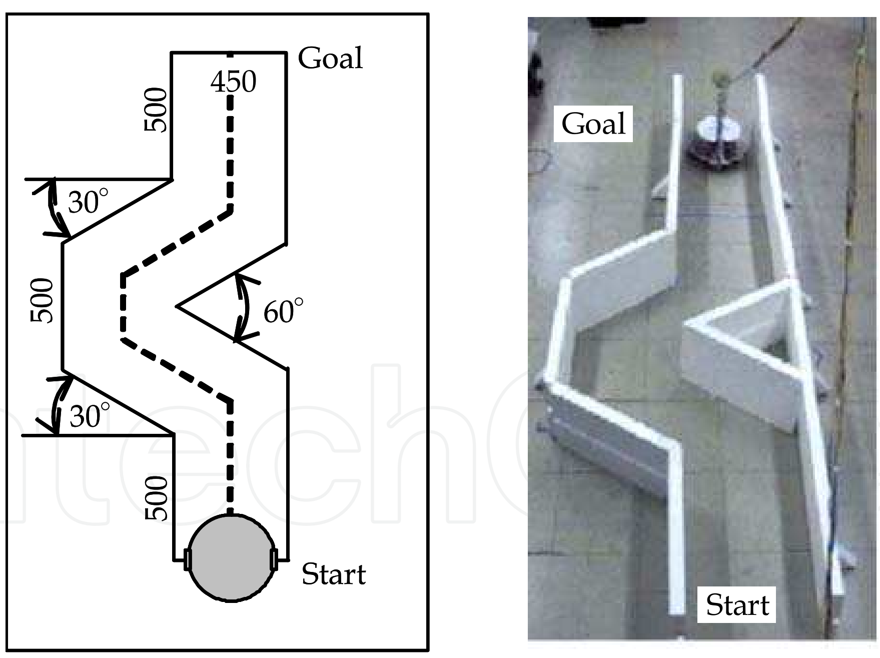

Fig. 6. Experimental environment

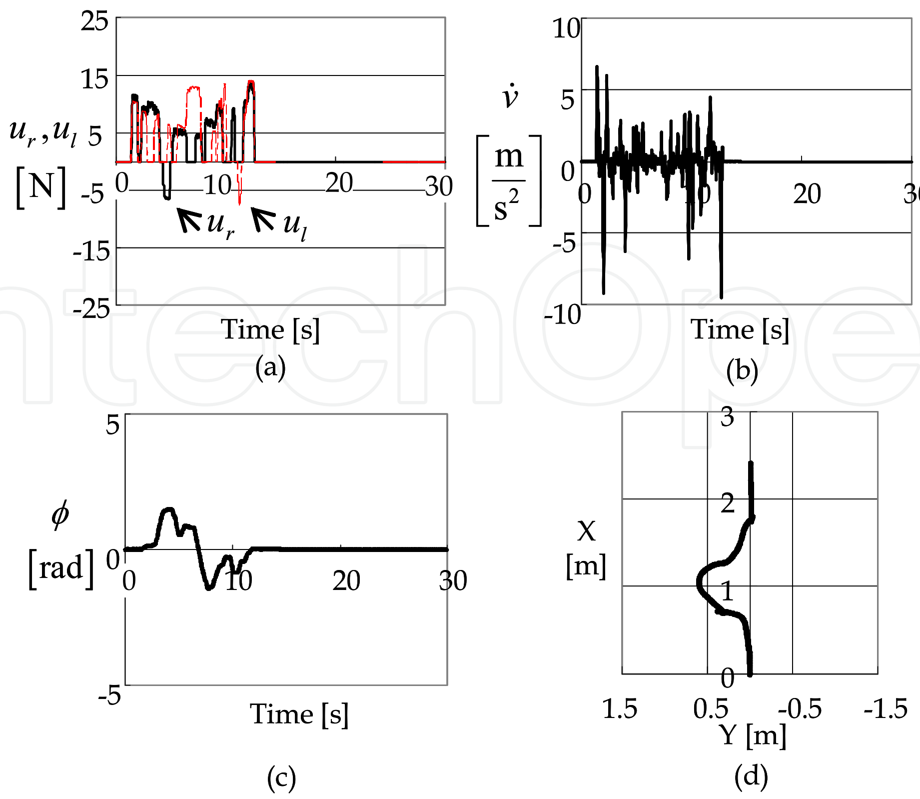

Fig. 7. Experimental results (Manual control)

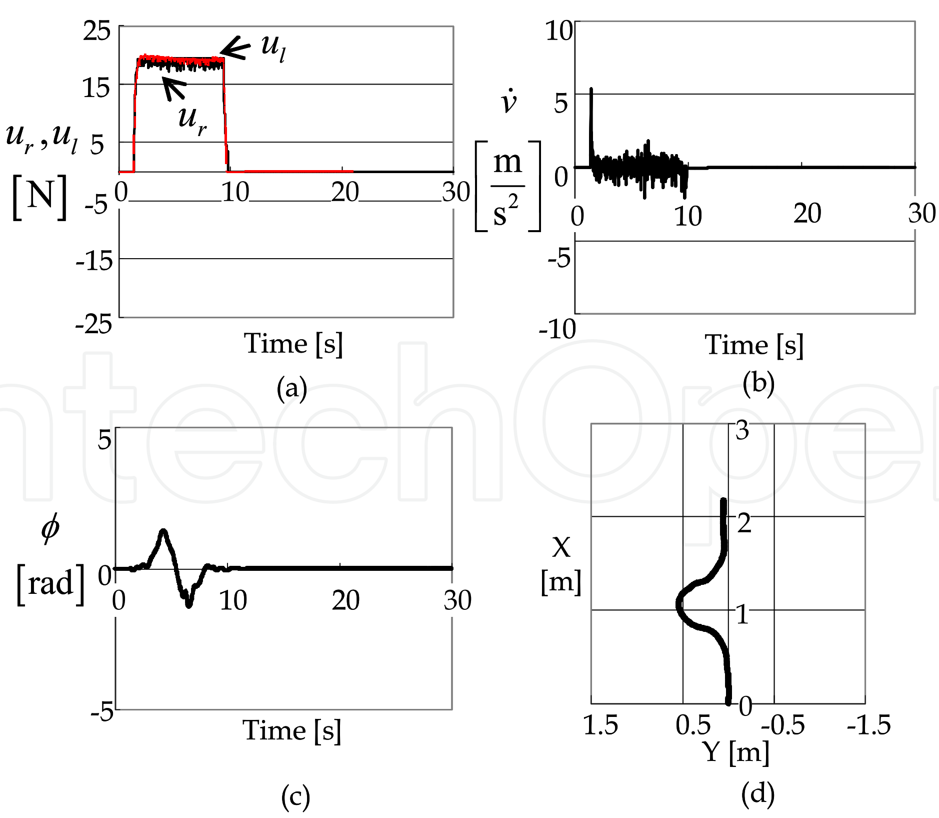

Fig. 8. Experimental results (Obstacle avoidance control)

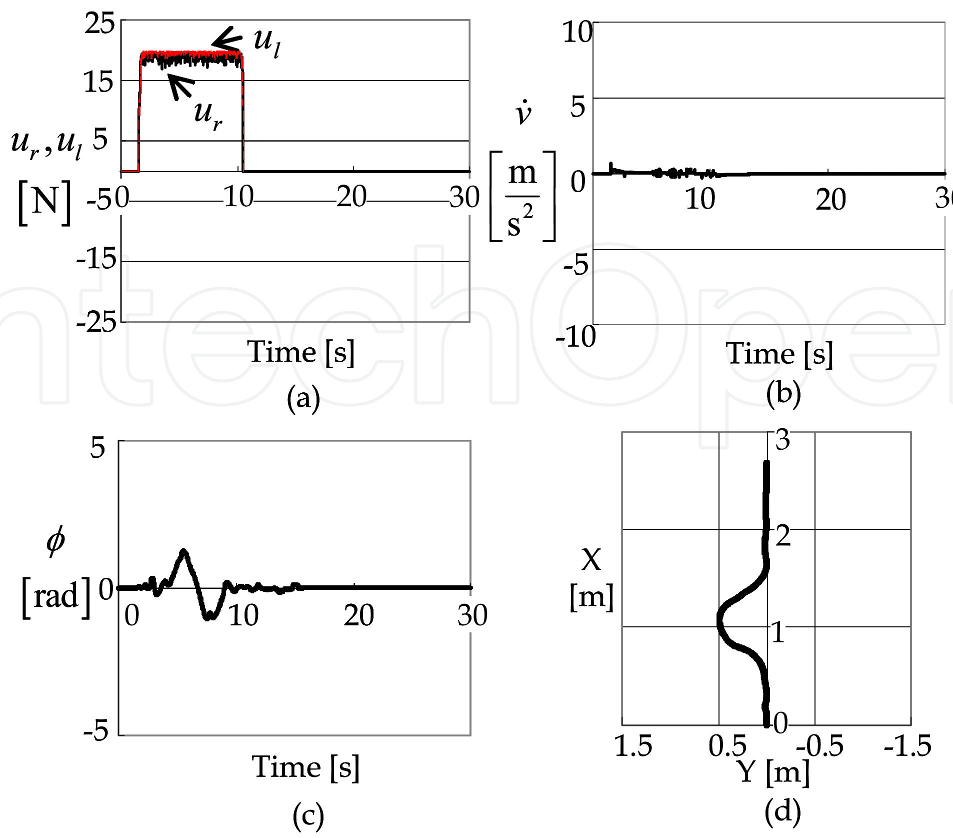

Fig. 9. Experimental results (Obstacle and tumble avoidance control)

○: Not occur, ×: Occur

Operator's No.	(a1) Manual control		(a2) Obstacle avoidance		(a3) Obstacle and tumble avoidance	
	Collision	Tumble	Collision	Tumble	Collision	Tumble
1	×	×	○	×	○	○
2	○	×	○	○	○	○
3	×	×	○	×	○	○
4	○	×	○	○	○	○
5	○	×	○	○	○	○
6	○	×	○	○	○	○
7	○	×	○	×	○	○
8	○	○	○	○	○	○
9	○	○	○	×	○	○
10	○	○	○	×	○	○

Table 2. Summary of experimental results

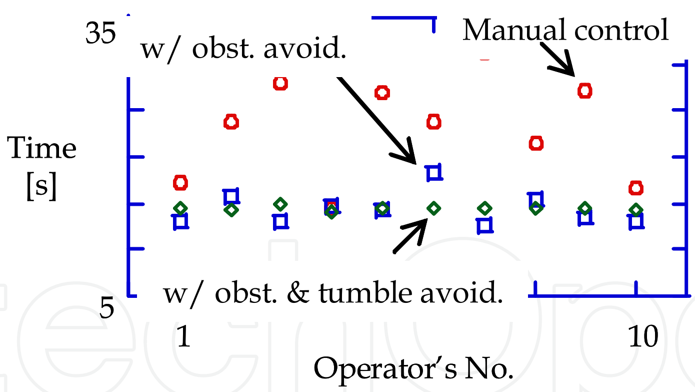

Fig. 10. Required time to pass through course

5. Conclusion

This chapter presents a model reference control approach for a human-operated mobile robot that transports an object. This type of robot has wide applications in industrial and household tasks. The operational easiness of the robot is verified by experiments where operators are required to operate the robot with a transported object to pass through a corridor-like space. Because even young students failed to operate the robot, a function to support the operation is obviously required. The operational easiness is improved by the proposed approach, with which all operators succeeded in transporting the object without collision nor tumble of the object.

6. References

Anderson, R. J. & Spong, M. W. (1989). Bilateral Control of Teleoperators with Time Delay, *IEEE Trans. Automatic Control*, Vol. 34, No. 5, pp. 494-501.

Bettini, A.; Marayong, P.; Lang, S.; Okamura, A. M. & Hager, G. D. (2001). Vison-Assisted Control for Manipulation Using Virtual Fixtures, *IEEE Trans. Robotics and Automation*, Vol. 20, No. 6, pp. 953-966.

Bonnafous, F., D. & Lefebvre, O. (2004). Reactive Path Deformation for Nonholonomic Mobile Robots, *IEEE Trans. Robotics and Automation*, Vol. 20 No. 6 pp. 967-977.

Fox, D., Burgard, W. & Thrun, S. (1997). The Dynamic Window Approach to Collision Avoidance, *IEEE Robotics and Automation Magazine*, Vol. 4, pp. 23-33.

Kazerooni, H. & Steger, R. (2006). The Berkeley Lower Extremity Exoskeleton, *ASME J. Dyn. Syst. Meas., Control*, Vol. 128, No. 1, pp. 14-25.

Khatib, O. (1986). Real-Time Obstacle Avoidance for Manipulators and Mobile Robots, *Int. J. Robotics Research*, Vol. 5, No. 1, pp. 90-98.

Lawrence, D. A. (1993). Stability and Transparency in Bilateral Teleoperation, *IEEE Trans. Robotics and Automation*, Vol. 9, No. 5, pp. 624-637.

Ö gren, P. & Leonard, N. E. (2005). A Convergent Dynamic Window Approach to Obstacle Avoidance, *IEEE Trans. Robotics and Automation*, Vol. 21, No. 2, pp. 188-195.

Peshkin , M. A.; Colgate J. E.; Wannasuphoprasit W.; Moore C. A.; Gillespie B. & Akella P. (2001). Cobot Architecture, *IEEE Trans. Robotics and Automation*, Vol. 17, No. 4, pp. 377-390.

Factory Automation
Edited by Javier Silvestre-Blanes

ISBN 978-953-307-024-7
Hard cover, 602 pages
Publisher InTech
Published online 01, March, 2010
Published in print edition March, 2010

Factory automation has evolved significantly in the last few decades, and is today a complex, interdisciplinary, scientific area. In this book a selection of papers on topics related to factory automation is presented, covering a broad spectrum, so that the reader may become familiar with the various fields, and also study them in more depth where required. Within various chapters in this book, special attention is given to distributed applications and their use of networks, since it is one of the most relevant subjects in the evolution of factory automation. Different Medium Access Control and networks are analyzed, while Ethernet and Wireless networks are looked at in more detail, since they are among the hottest topics in recent research. Another important subject is everything concerning the increase in the complexity of factory automation, and the need for flexibility and interoperability. Finally the use of multi-agent systems, advanced control, formal methods, or the application in this field of RFID, are additional examples of the ideas and disciplines that experts around the world have analyzed in their work.